

---

---

# Detection of interstellar radio recombination lines with NenuFAR

**Lucie Cros<sup>1,2</sup>, 1st year PhD student**  
Antoine Gusdorf<sup>1,2</sup>, Philippe Salomé<sup>2</sup>, Sergey Stepkin<sup>3</sup>  
Philippe Zarka<sup>4</sup>, Alan Loh<sup>4</sup>, Pedro Salas<sup>5</sup>, Pierre Lesaffre<sup>1</sup>

---

<sup>1</sup>Laboratoire de Physique de l'École Normale Supérieure, ENS, Université PSL, CNRS, Sorbonne Université, Université Paris Cité, Paris

<sup>2</sup>LERMA, Observatoire de Paris, Université PSL, Sorbonne Université, 75014 Paris, France

<sup>3</sup>Institute of Radio Astronomy NAS of Ukraine, 4, Mystetstv St., Kharkiv, 61002, Ukraine

<sup>4</sup>LESIA, Observatoire de Paris, Université PSL, Sorbonne Université, 75014 Paris, France

<sup>5</sup>Green Bank Observatory, Green Bank, WV 24944, USA

# Goal

→ Characterisation of the **diffuse ISM phase**.

## ➤ Scientific context

- The cycle of matter in the ISM
- Advantages of Carbon RRLs
- Sources

## ➤ Data reduction

- NenuFAR, its obstacles, and how to tackle them

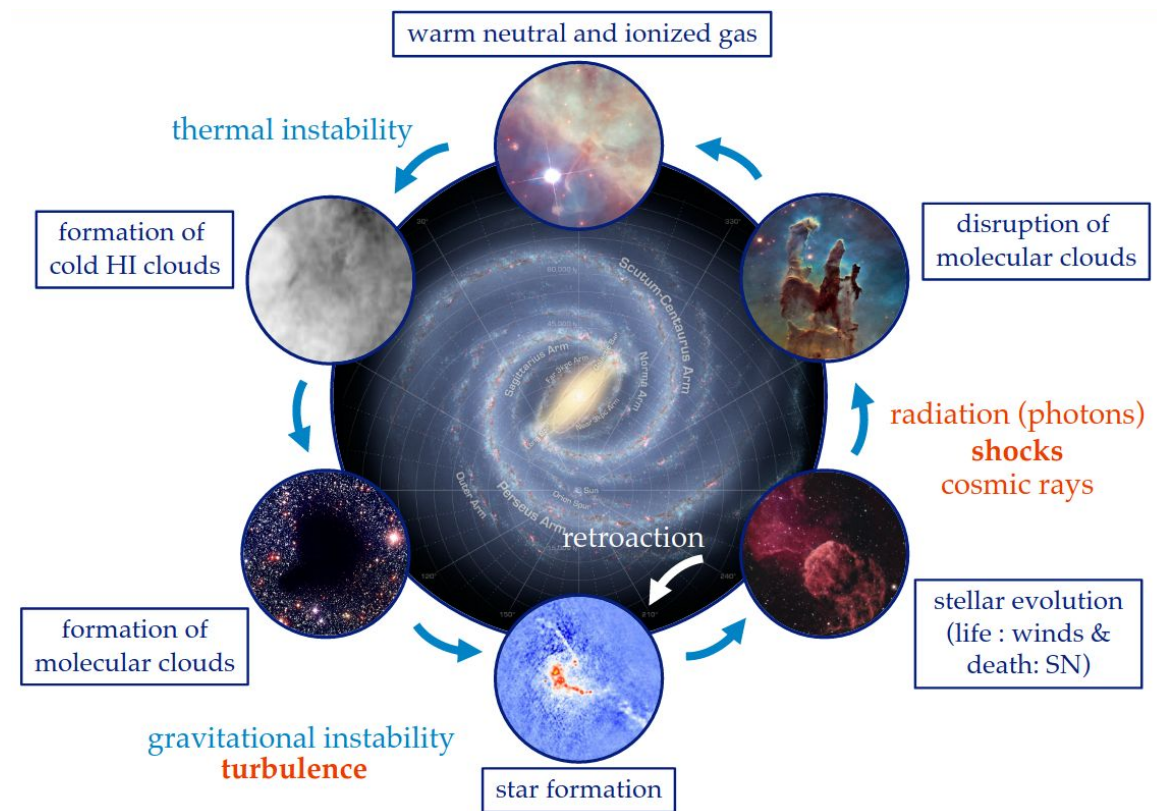
## ➤ First results

- Line detection
- From line fitting to physical constraints

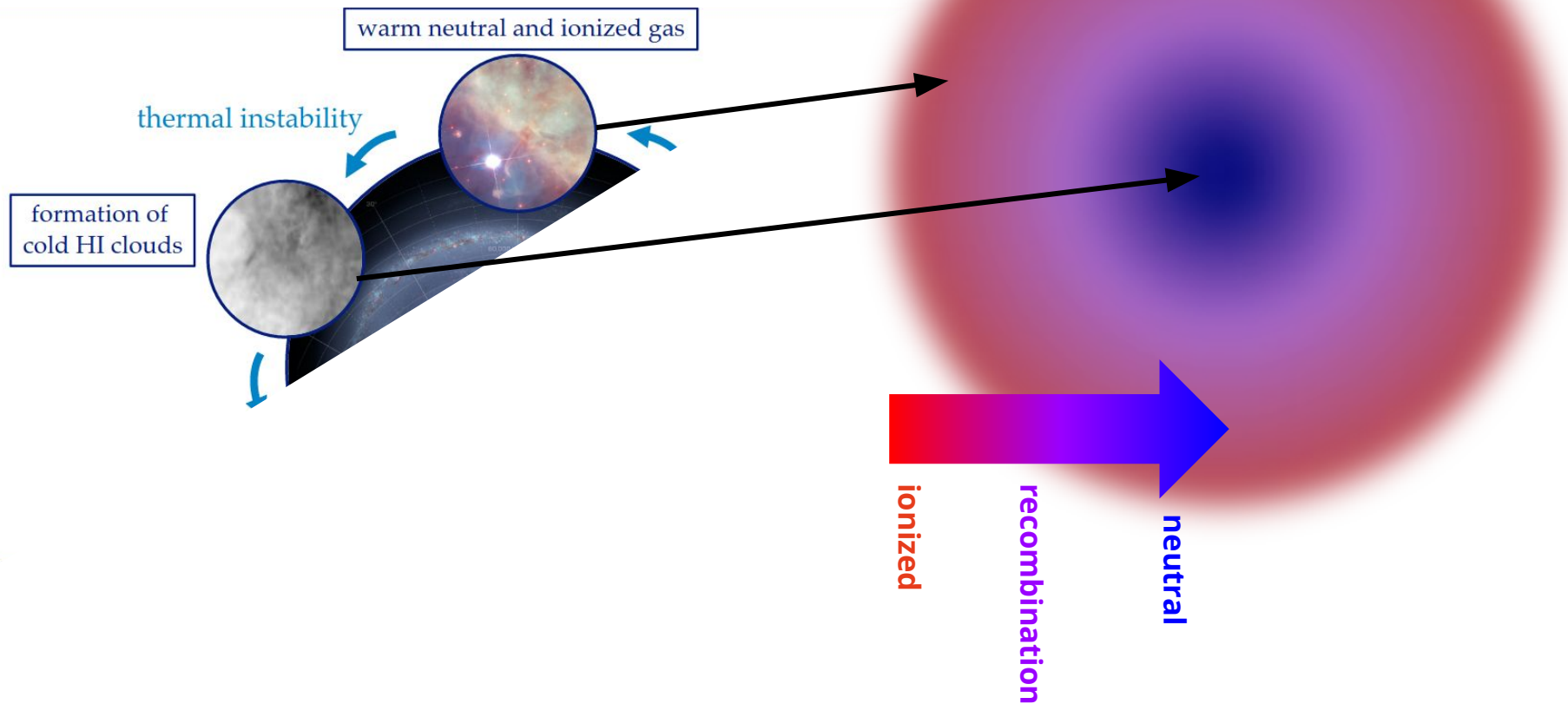
## ➤ Next ?

- Perspectives for the RRL team of NenuFAR

# Cycle of matter in the Interstellar Medium



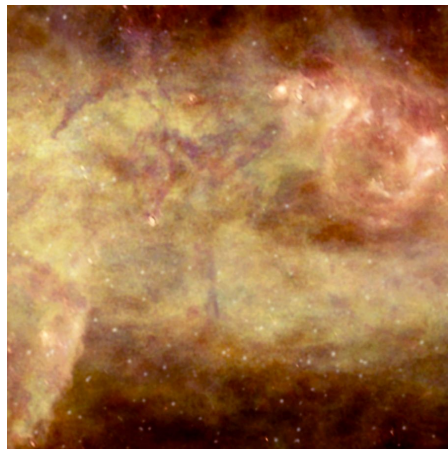
# Diffuse phase



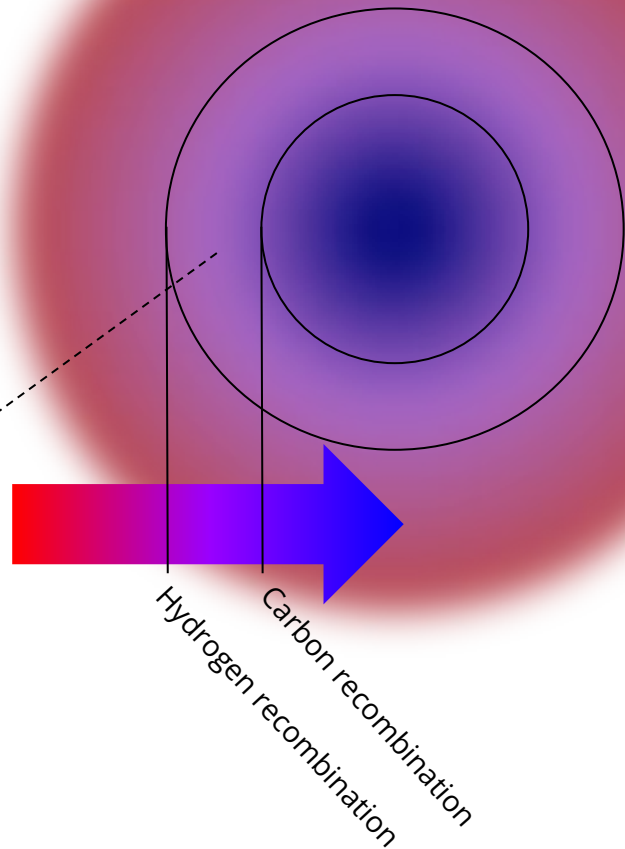
# Carbon Radio Recombination Lines

- $E_0(\text{H}) = -13.6 \text{ eV}$
- $E_0(\text{C}) = -11.2 \text{ eV}$

⇒  $\text{C}^+$  in HI region



21-cm map of the Perseus arm  
J. English : Canadian galactic plane survey



# Carbon Radio Recombination Lines

- $E_0(\text{H}) = -13.6 \text{ eV}$
- $E_0(\text{C}) = -11.2 \text{ eV}$

⇒  $\text{C}^+$  in HI region

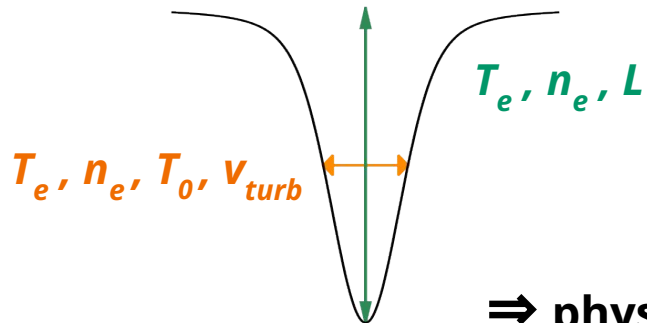
At high  $n$  :  $0 < T_x < T_{bg}$   
 ⇒ line in **absorption**

*Salgado et. al 2017*

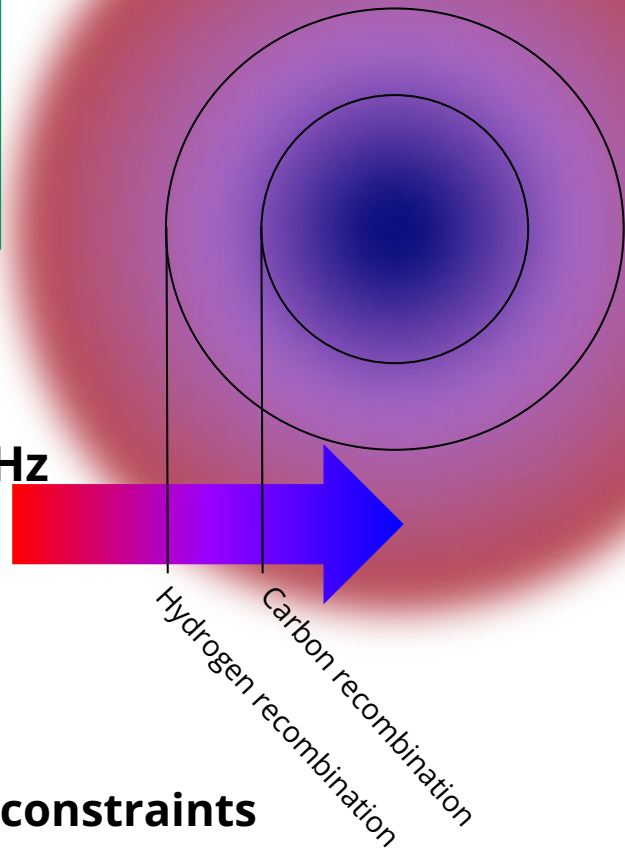
$\text{C}\alpha(n)$  transition for  $n \in [400, 850]$  ( $\Leftrightarrow [10, 85]$  MHz) :

$$\nu_{n+1 \rightarrow n} \propto \left( \frac{1}{n^2} - \frac{1}{(n+1)^2} \right) \simeq \frac{2}{n^3}$$

⇒ **450 lines in 70 MHz**



⇒ **physical/chemical constraints**



# Sources

| Source       | Type         | Coordinates<br>RA (J2000) Dec (J2000)     | Flux density at 50 MHz<br>[Jy] | Size arcmin<br>[arcmin] | Velocity components<br>[km/s] |
|--------------|--------------|---|--------------------------------|-------------------------|-------------------------------|
| Cassiopeia A | SNR          | $23^h 23^m 27.94^s + 58^\circ 48' 42.4''$ | 27 104                         | 7.4                     | -47, -38, 0                   |
| Cygnus A     | Radio galaxy | $19^h 59^m 28.35^s + 40^\circ 44' 02.1''$ | 22 146                         | 2.3                     | 4                             |
| Taurus A     | SNR          | $05^h 34^m 31.97^s + 22^\circ 00' 52.1''$ | 2 008                          | 7.9                     | 14                            |

# NenuFAR (Nancay Observatory)

Standalone radiotelescope + LOFAR extension + SKA pathfinder



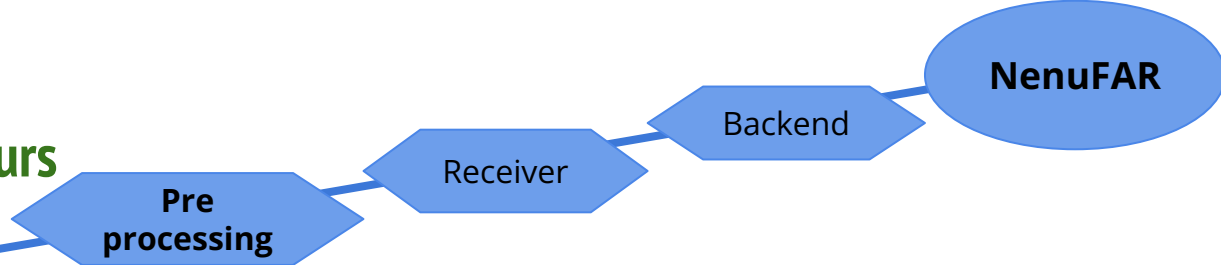
## EXPERIMENTAL SETUP

- ~80 mini-array of 19 antennas
- Frequency range : [10, 85] MHz
- spectral resolution **df ~ 95 Hz**
- spatial resolution ~ 1°
  
- KP10 : Radio Recombination Lines
- Beamforming mode



# Processing of data

example : Cassiopeia A, 2 hours



## Baseline flattening and RFI mitigation

### 2.a) Lane by lane

#### Time integration

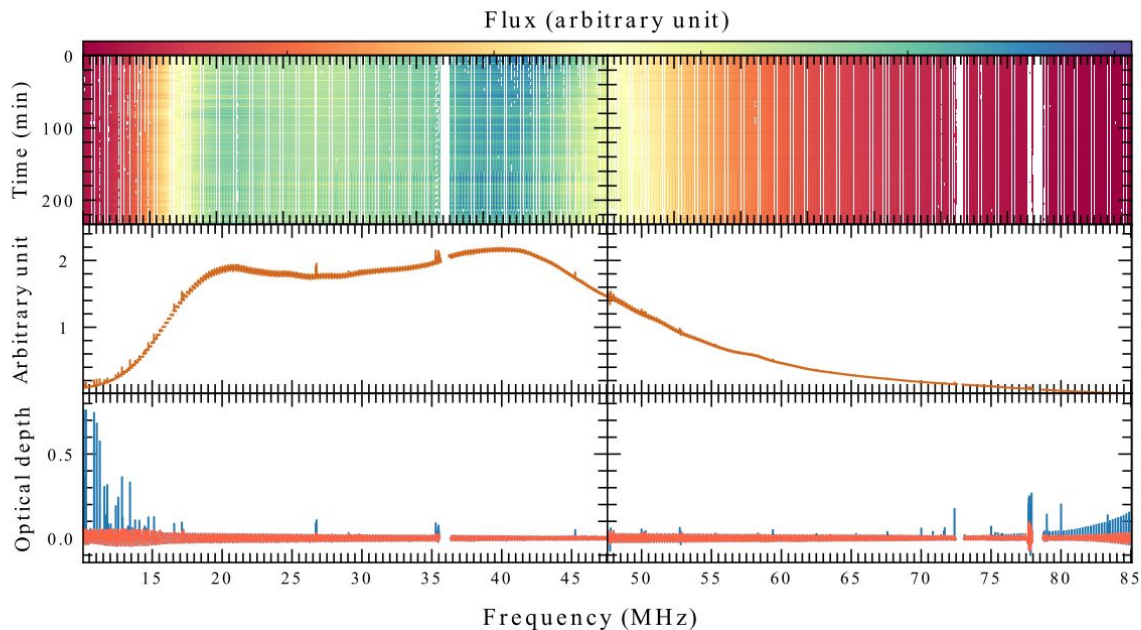
\* Weighted average of Stokes I

#### Flattening

\*  $\frac{I}{I_{smooth}} - 1$  with  $I_{smooth}$  from rebinned  $I$

#### RFI mitigation

\* recursive  $\sigma$  clipping



=> 2 lanes, 384 subbands, 786432 frequency channels

# Processing of data

example : Cassiopeia A, 2 hours

## 2.b) Subband by subband

### RFI mitigation 2 : narrow spikes

\*  $\sigma$  clipping based on subband gradient

### Flattening 2 : baseline S-shape

\* Individual subband shape inferred from the median of  $k$  neighboring subbands

### Mitigation 3 : broad spikes, outside lines

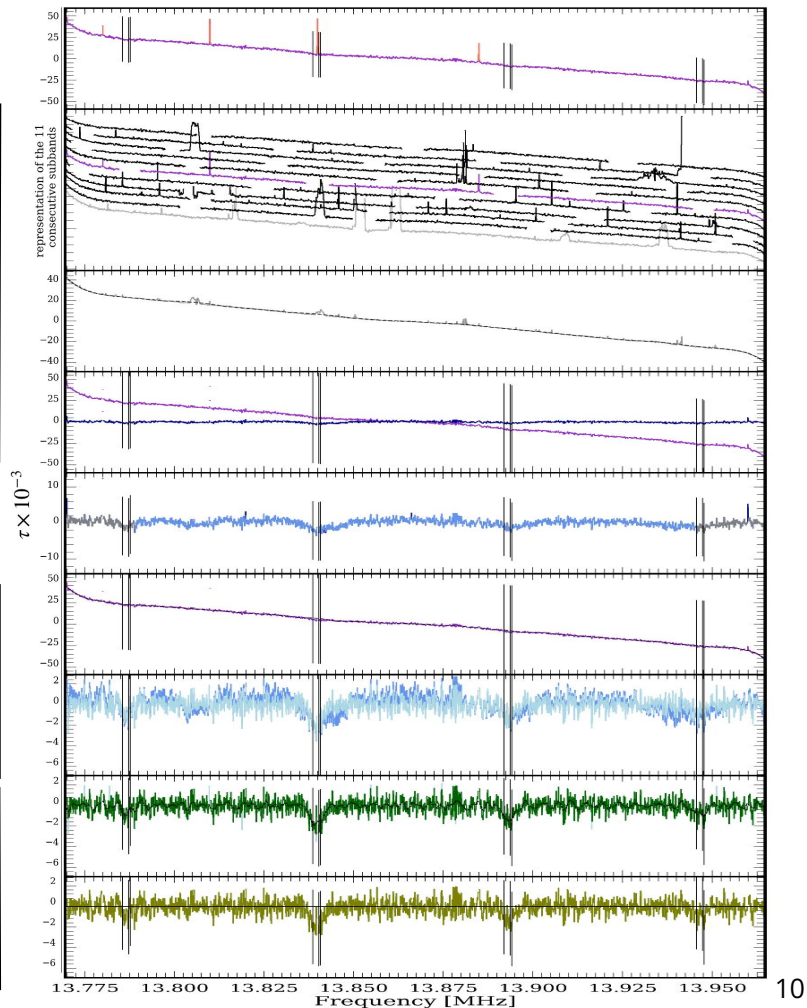
\* Mask around expected lines  
\* recursive  $\sigma$  clipping based on masked subband

### Flattening 3 : residual baseline variation

\* Smoothing with a SavGol filter of the masked subband to find and remove residual variation.

### RFI mitigation 4 : inside masked lines

\* Flattening of lines with a SavGol filter  
\* recursive  $\sigma$  clipping based on the flattened subband.



# Processing of data

example : Cassiopeia A, 2 hours

## 2.c) Whole spectrum

### RFI mitigation 5

\* recursive  $\sigma$  clipping based on line free spectrum

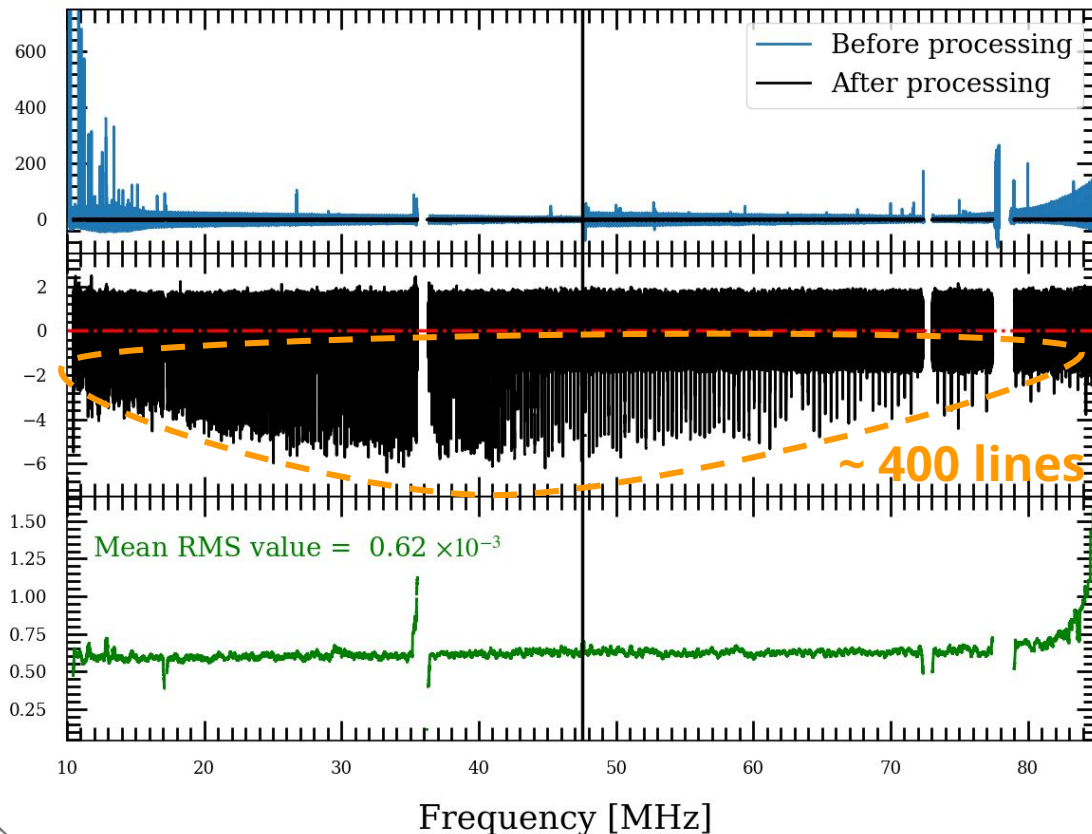
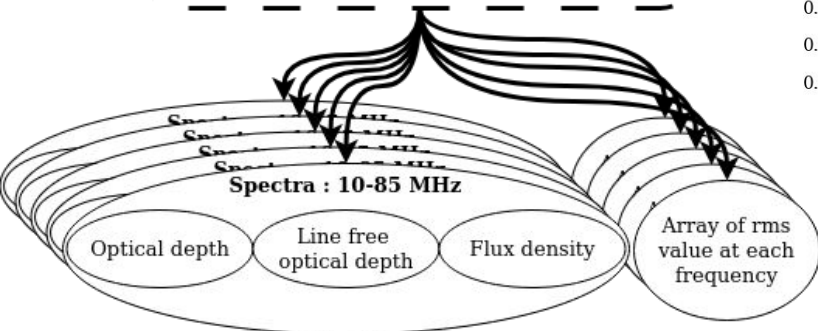
### Source continuum emission

\* Computation of flux density based on analytical modeling for source continuum when available

### RMS computation

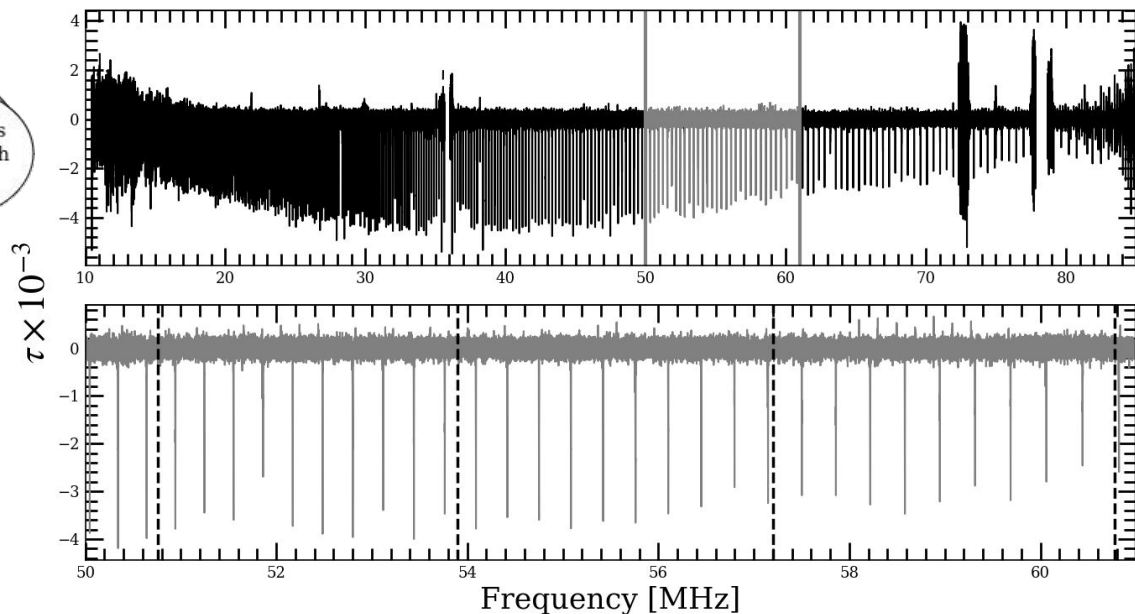
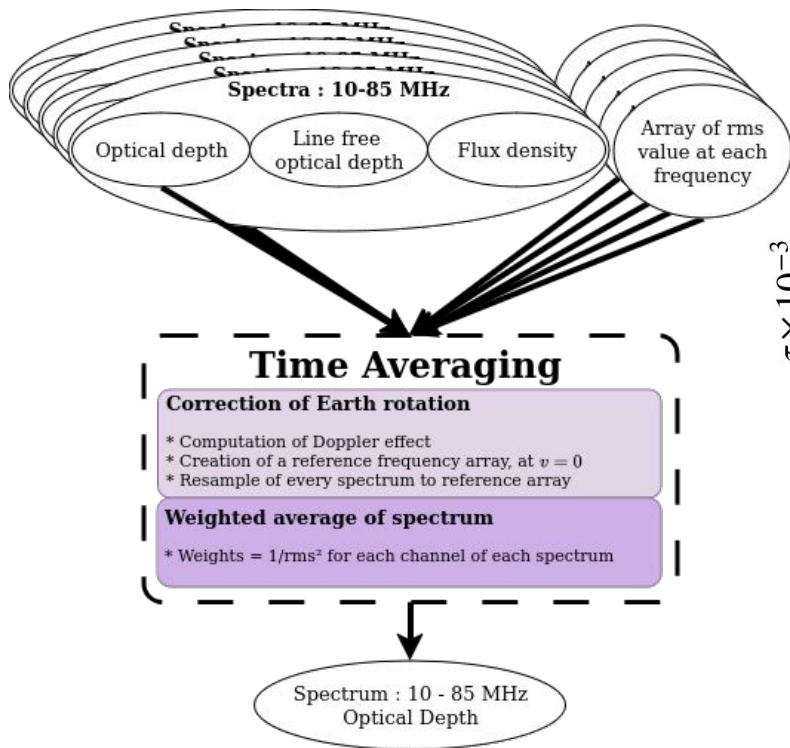
\* For each frequency channel : RMS estimate over sliding window of subband width

$\tau \times 10^{-3}$



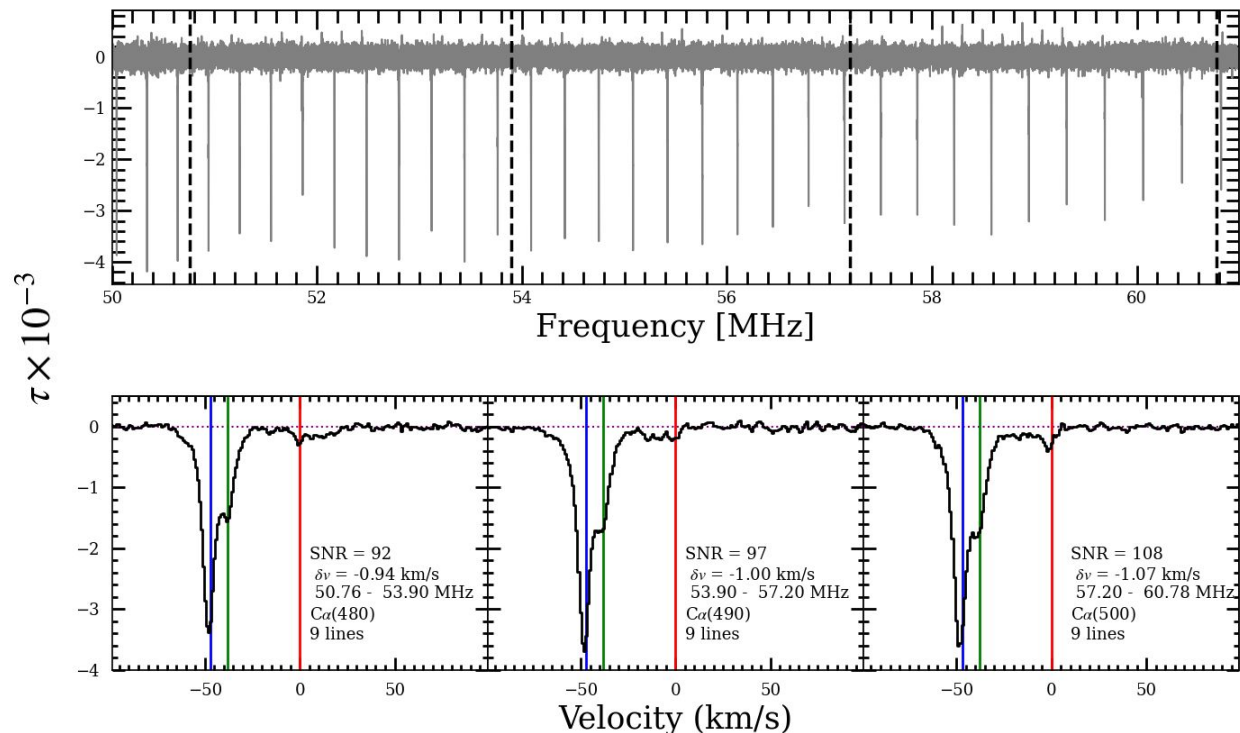
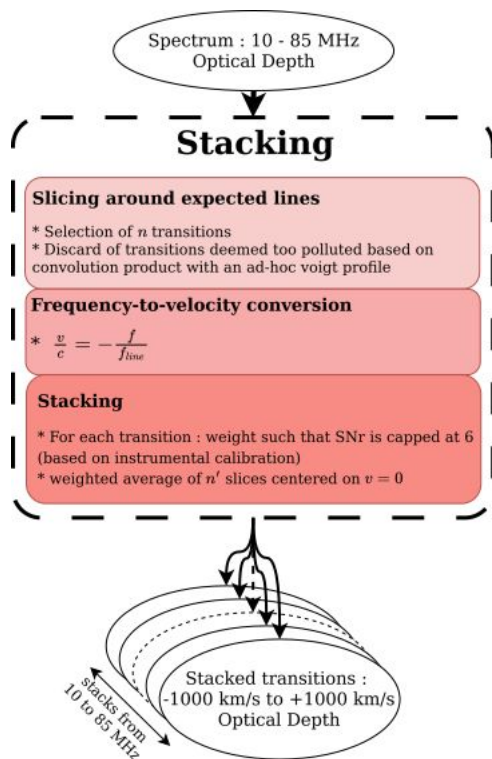
# Processing of data

example : Cassiopeia A, 71 hours



# Processing of data

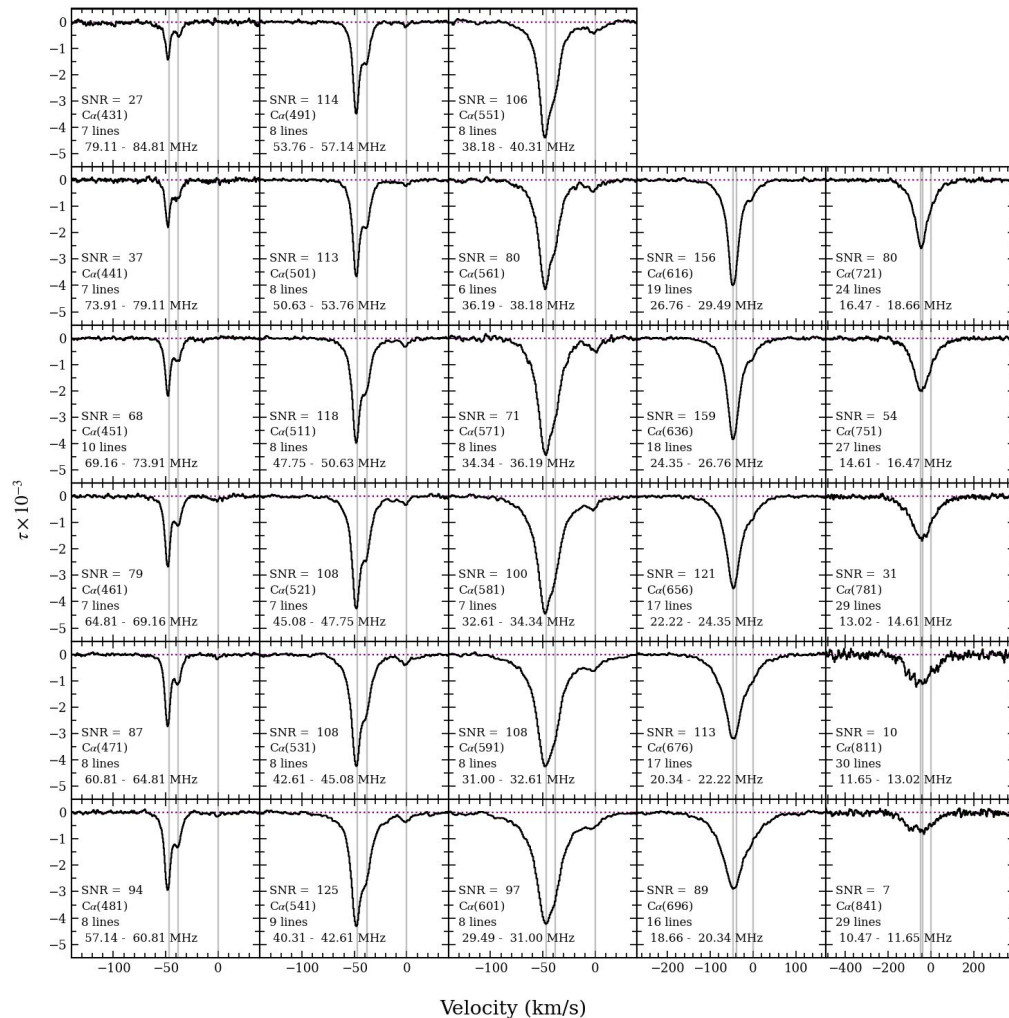
example : Cassiopeia A, 71 hours



=> 3 velocity components : -47, -38 and 0 km/s<sub>3</sub>

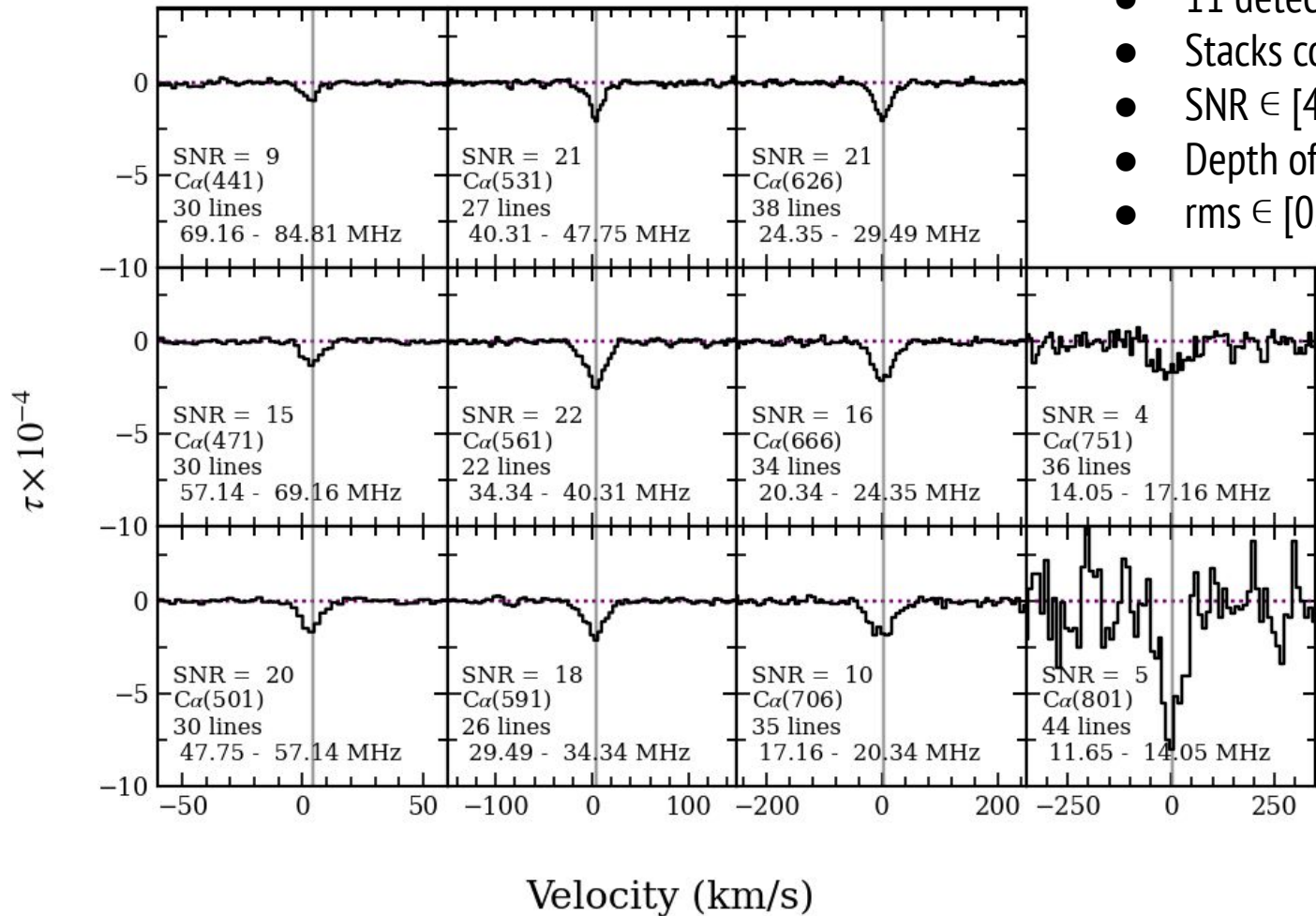
# Detections

| <b>Source</b> | <b>On-source time (hours)</b> | <b>Expected velocity components (km/s)</b> | <b>Number of detection</b> | <b>Typical value of optical depth</b> | <b>Mean value of SNr</b> |
|---------------|-------------------------------|--|----------------------------|---------------------------------------|--------------------------|
| Cas A         | 71.5                          | -47, -38, 0                                | 28                         | $10^{-3}$                             | 88                       |
| Cyg A         | 157.5                         | 4  | 11                         | $10^{-4}$                             | 15                       |
| Tau A         | 104                           | 14   | 17                         | $10^{-4}$                             | 13                       |



## CASSIOPEIA A

- 28 detections at  $3\sigma$  threshold
- Stacks contains 7 to 30 lines
- $\text{SNR} \in [7, 159]$
- Depth of line  $\in [0.8, 4.4] \times 10^{-3}$
- $\text{rms} \in [2.4, 12.2] \times 10^{-5}$

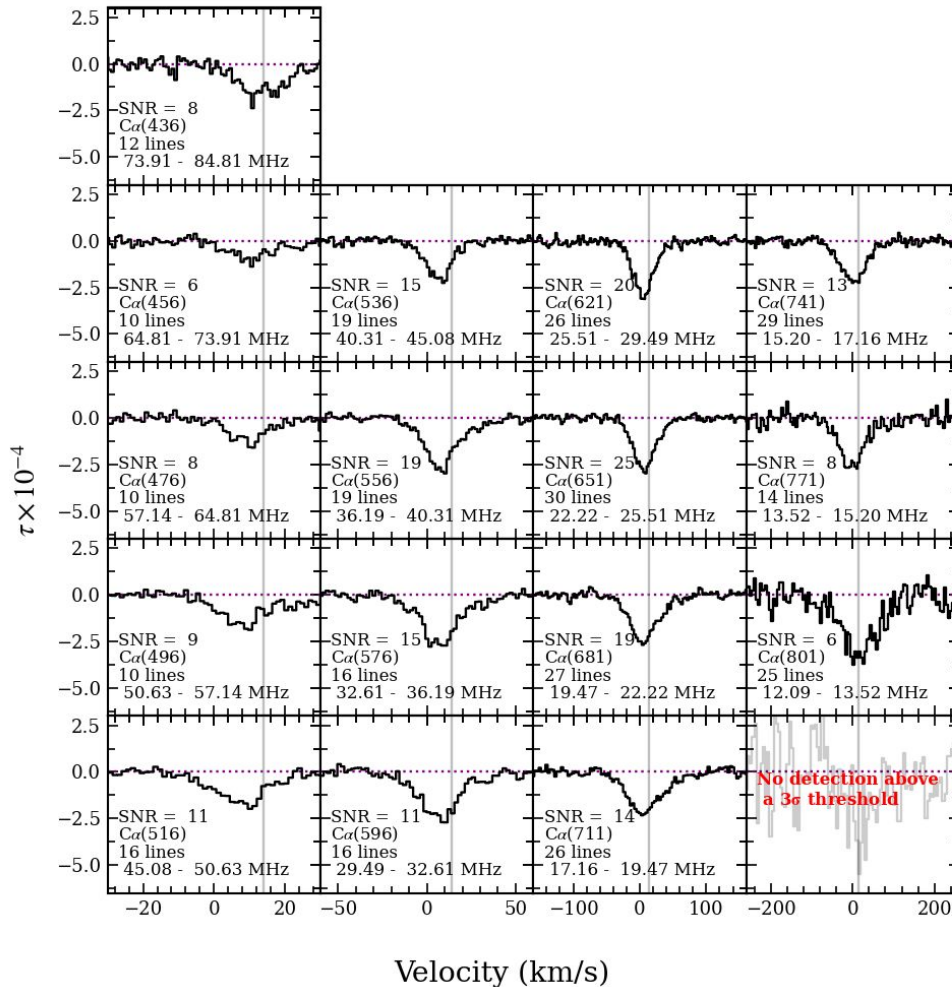


- 11 detections at  $3\sigma$  threshold
- Stacks contains 22 to 44 lines
- $\text{SNR} \in [4, 22]$
- Depth of line  $\in [0.9, 8.8] \times 10^{-4}$
- $\text{rms} \in [0.8, 1.6] \times 10^{-5}$

**CYGNUS A**



## TAURUS A



- 16 detections at  $3\sigma$  threshold
- Stacks contains 10 to 30 lines
- $\text{SNR} \in [6, 25]$
- Depth of line  $\in [1.3, 5.4] \times 10^{-4}$
- $\text{rms} \in [1.2, 17.3] \times 10^{-5}$

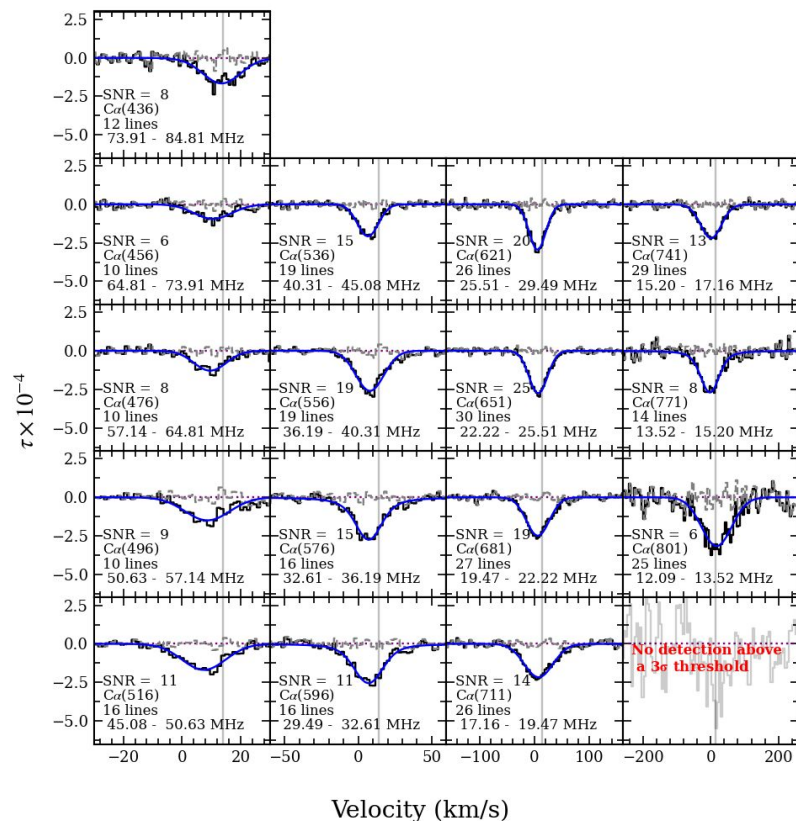
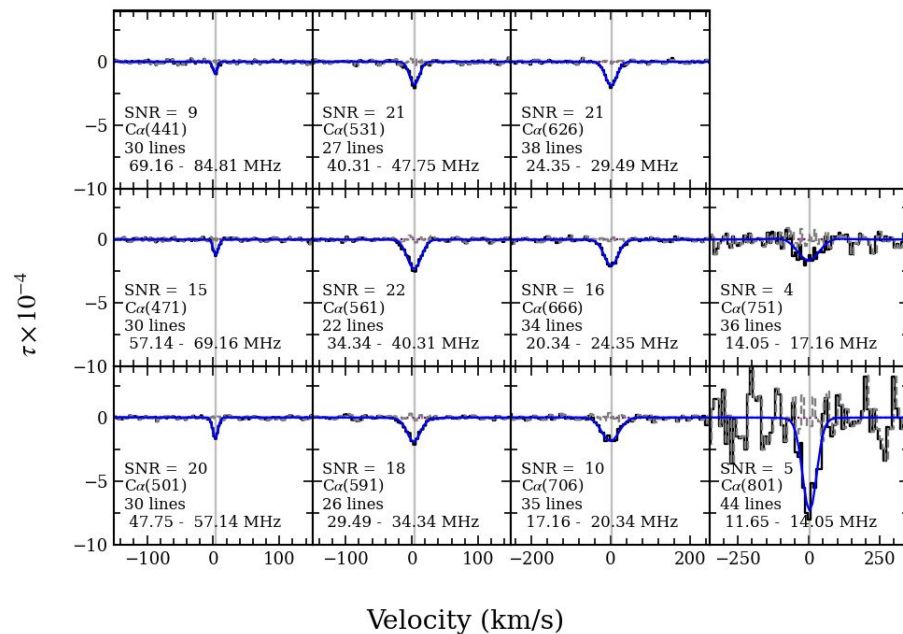
# Inferring physical parameters of the local ISM

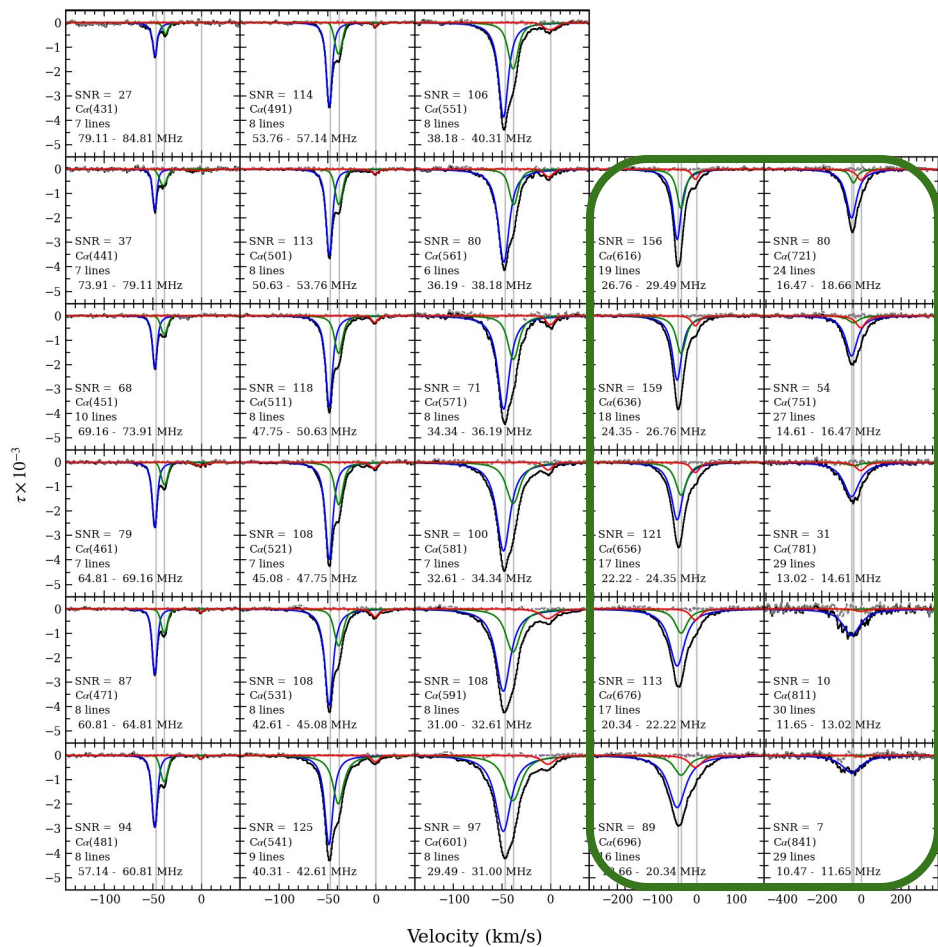
## => Methodology

1. Fitting a voigt profile on each line
  - inferring the **FWHM ( $w$ )** and the **integrated intensity ( $I$ )** for each transition: we get a set of  $w(n)$  and  $I(n)$ .
2. Modeling the **variation** of  $w$  and  $I$  as a function the principal quantum number of each transitions  $n$ .
3. Fitting the observed  $w(n)$  and  $I(n)$  with the **theoretical modelings**  $w_{\text{th}}(n)$   
 $\int I, \Delta v_L$  and  $\Delta v_G$ .
  - inferring constraints on the physical parameters  $T_e, n_e, T_0, v_t, L$ .

# 1. Fitting the lines

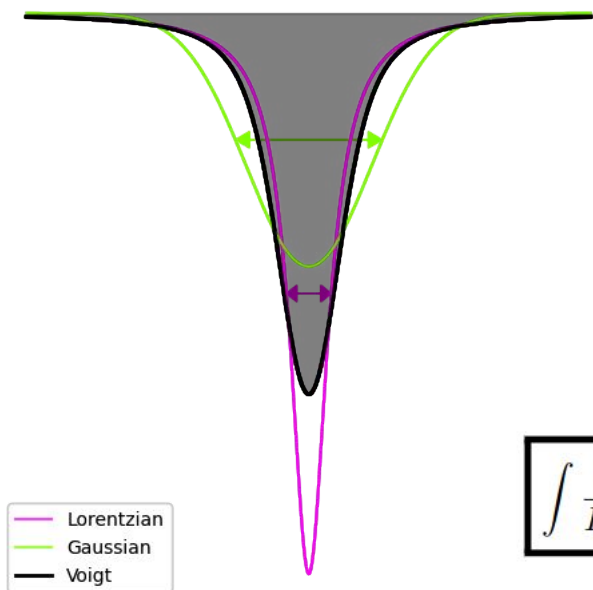
-> Method : *curve fit, scipy*





Blending of components  
=> less confidence in the  
results of the fits

## 2. Modeling the transitions



$$\Delta\nu_G = \frac{\nu_{n \rightarrow n+1}}{c} \sqrt{\frac{2k_B T_e}{m_C} + \langle v_{turb} \rangle^2}$$

$$\Delta\nu_{natural} = \frac{1.2 \cdot 10^{-6} \ln n}{n^2} \nu_{n \rightarrow n+1}$$

$$\Delta\nu_{pressure} = \frac{1}{2\pi} n_e 10^{a(T_e)} n^{\gamma(T_e)} \text{ Hz}$$

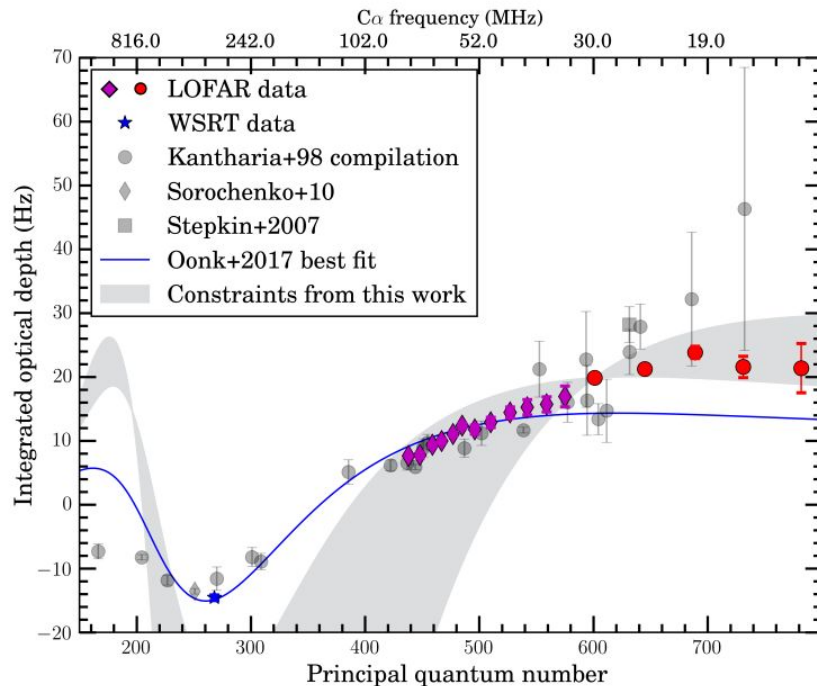
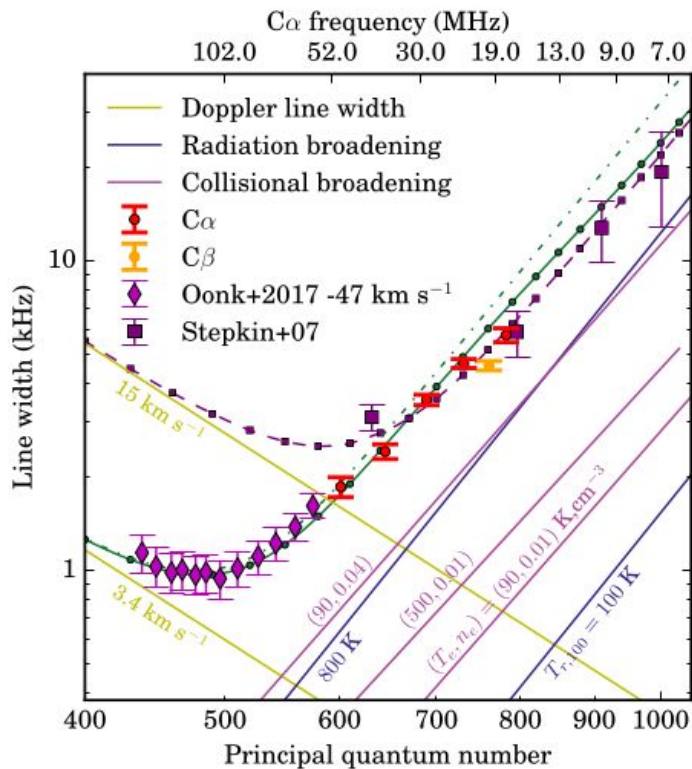
$$\Delta\nu_{radiation} = \frac{6.096 \times 10^{-17}}{2\pi} T_0 n^{5.8} \text{ Hz}$$

$$\int \frac{I_\nu}{I_\nu^{cont}} = -0.2 b_n(n_e, T_e) \beta_{n, n+\Delta n}(n_e, T_e) \left( \frac{T_e}{100 \text{ K}} \right)^{-2.5} \left( \frac{n_e}{0.1 \text{ cm}^{-3}} \right)^2 \left( \frac{L}{\text{pc}} \right) \text{ Hz}$$

$$T_e, n_e, v_{turb}, T_0, L$$

Gordon & Sorochenko, 2009  
Salgado et al, 2017

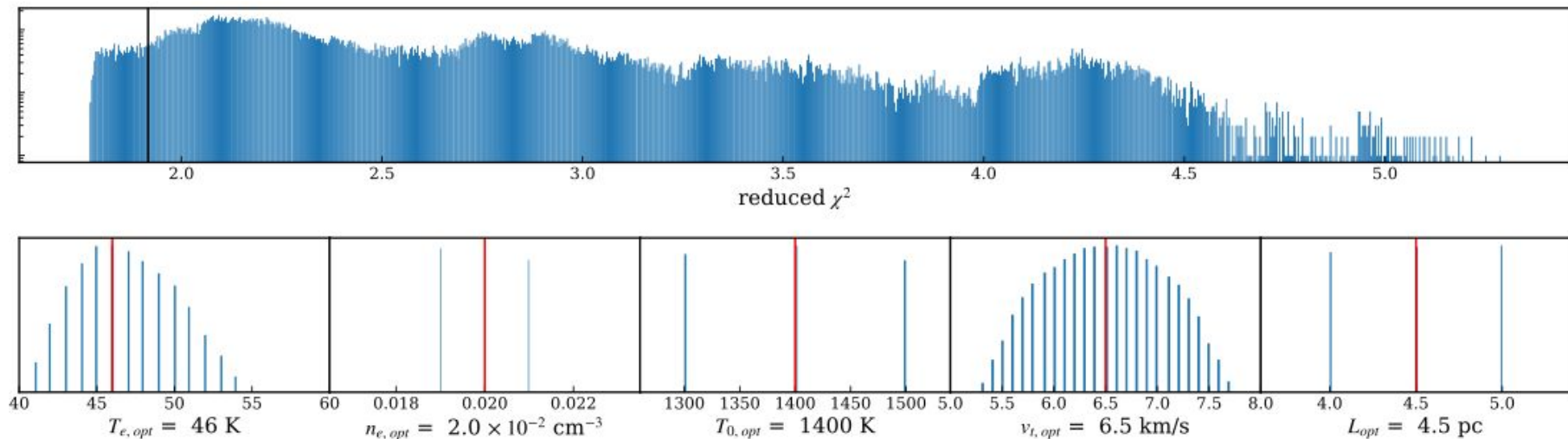
## 2. Broadening and intensity as a function of quantum number



Salas et al, 2017

### 3. Fitting the variation of $w$ and $l$ as a function of $n$ -> Method : minimisation of reduced $\chi^2$ on a 5D grid

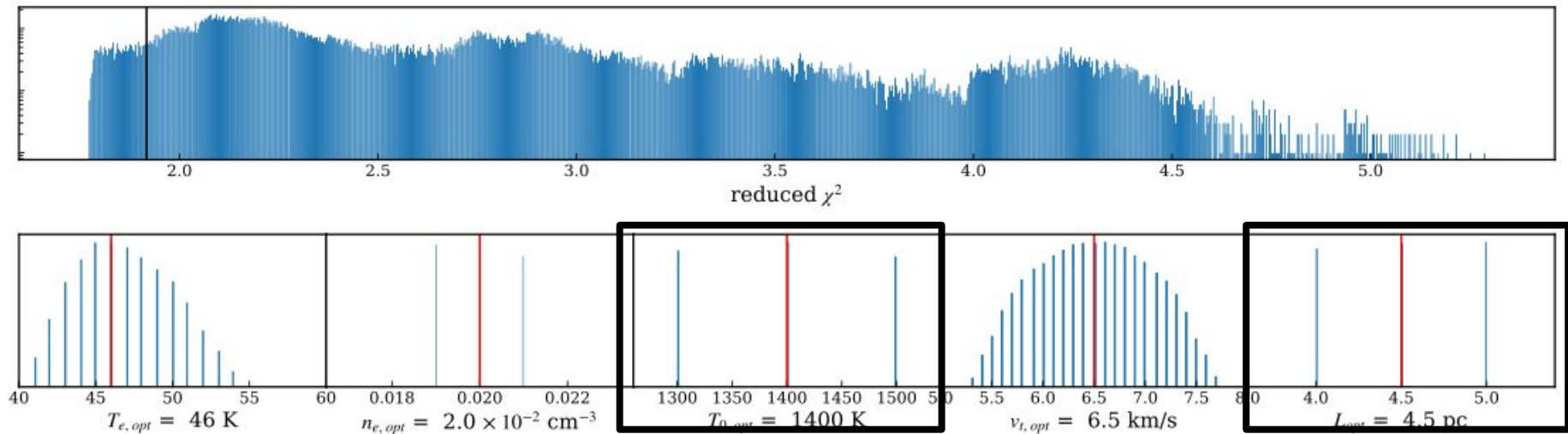
Optimal reduced  $\chi^2 = 1.77$



Example for *Cygnus A*. Uncertainties are evaluated as the fifth percentile of the reduced  $\chi^2$  on the grid

### 3. Fitting the variation of $w$ and $l$ as a function of $n$ -> Method : minimisation of reduced $\chi^2$ on a 5D grid

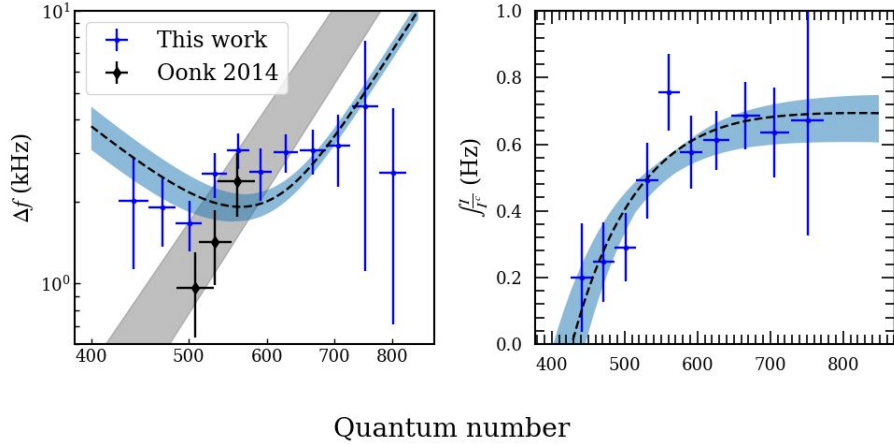
Optimal reduced  $\chi^2 = 1.77$



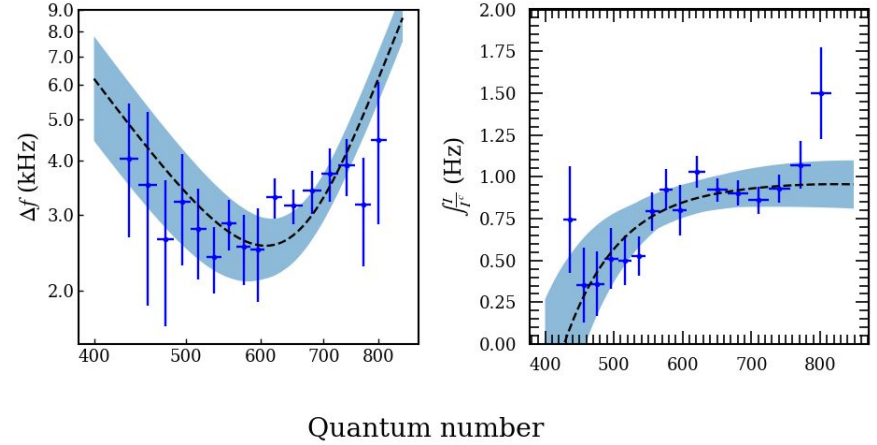
Example for *Cygnus A*. Uncertainties are evaluated as the first percentile of the reduced  $\chi^2$  on the grid



## Cygnus A

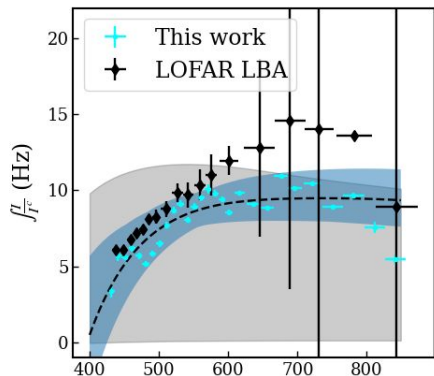
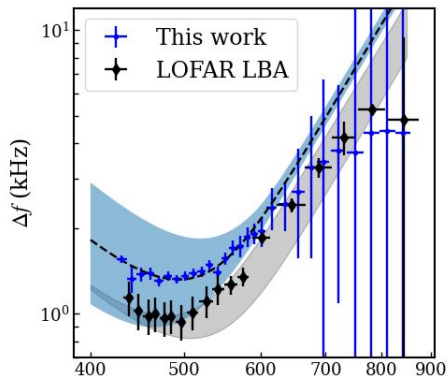


## Taurus A



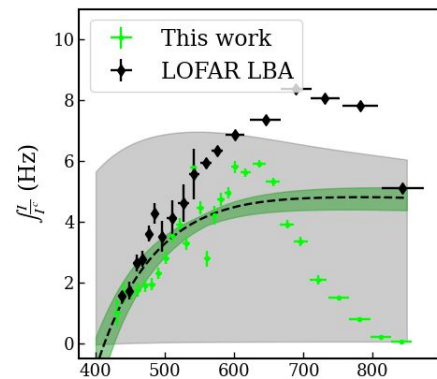
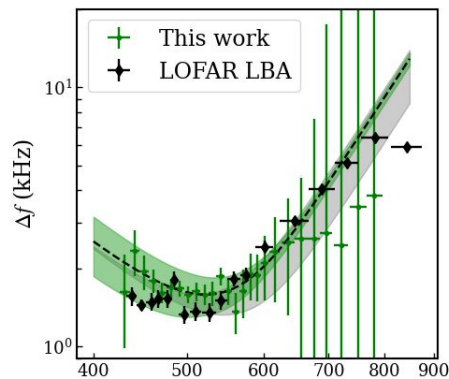
|               | $T_e$ (K)       | $n_e$ ( $\text{cm}^{-3}$ ) | $T_0$ (K)      | $v_t$ (km/s)         | L (pc)      |
|---------------|-----------------|----------------------------|----------------|----------------------|-------------|
| Cyg A NenuFAR | $46^{+8}_{-5}$  | $0.020^{+0.001}_{-0.001}$  | $1400 \pm 100$ | $6.5^{+1.2}_{-1.2}$  | $4 \pm 0.5$ |
| Cyg A LOFAR   | 50 - 500        | 0.005 - 0.070              | (2700)         | -                    | -           |
| Tau A NenuFAR | $34^{+13}_{-7}$ | $0.035^{+0.009}_{-0.005}$  | $1000 \pm 100$ | $10.8^{+2.8}_{-3.1}$ | $1 \pm 0.5$ |

## Cas A : -47 km/s



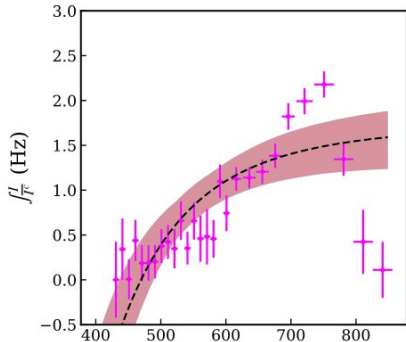
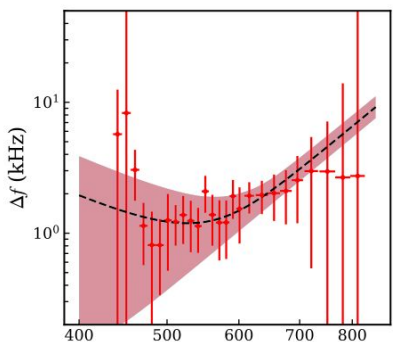
Quantum number

## Cas A : -38 km/s



Quantum number

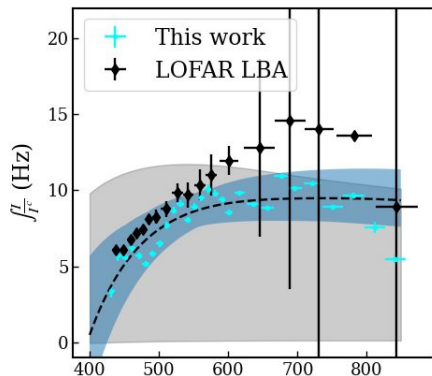
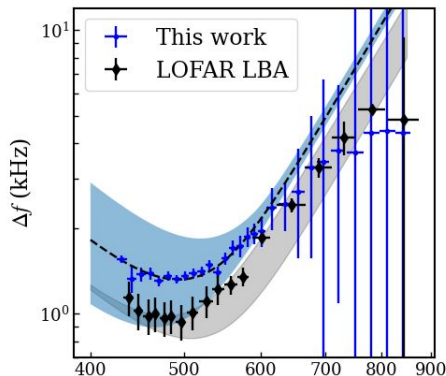
## Cas A : 0 km/s



Quantum number

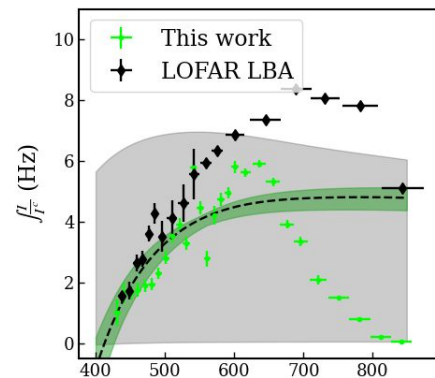
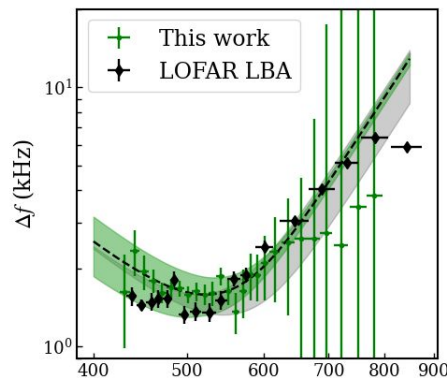
|                         | $T_e$ (K)       | $n_e$ ( $\text{cm}^{-3}$ ) | $T_0$ (K)      | $v_t$ (km/s)        | L (pc)         |
|-------------------------|-----------------|----------------------------|----------------|---------------------|----------------|
| <b>-47 km/s NenuFAR</b> | $39^{+7}_{-4}$  | $0.036^{+0.001}_{-0.001}$  | $2000 \pm 100$ | $3.0^{+1.2}_{-1.1}$ | $16 \pm 0.5$   |
| <b>-47 km/s LOFAR</b>   | $85 \pm 10$     | $0.040 \pm 0.005$          | $1351 \pm 83$  | $2.013 \pm 0.002$   | $35.3 \pm 1.2$ |
| <b>-38 km/s NenuFAR</b> | $43^{+4}_{-3}$  | $0.026^{+0.000}_{-0.001}$  | $1800 \pm 100$ | $4.3^{+1.1}_{-1.2}$ | $17 \pm 0.5$   |
| <b>-38 km/s LOFAR</b>   | $85 \pm 10$     | $0.040 \pm 0.005$          | $1507 \pm 128$ | $4.069 \pm 0.002$   | $18.6 \pm 1.6$ |
| <b>0 km/s</b>           | $16^{+11}_{-5}$ | $0.042^{+0.015}_{-0.016}$  | $1200 \pm 100$ | $3.0^{+1.2}_{-1.1}$ | $0.5 \pm 0.5$  |

## Cas A : -47 km/s



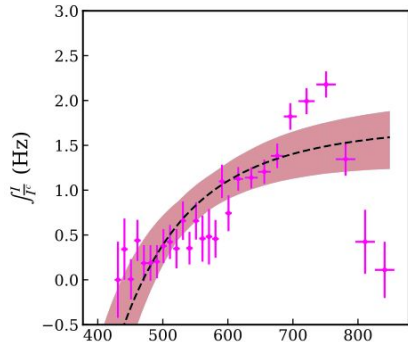
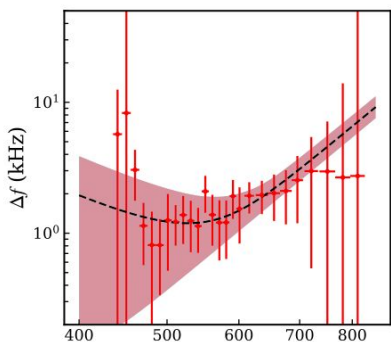
Quantum number

## Cas A : -38 km/s



Quantum number

## Cas A : 0 km/s



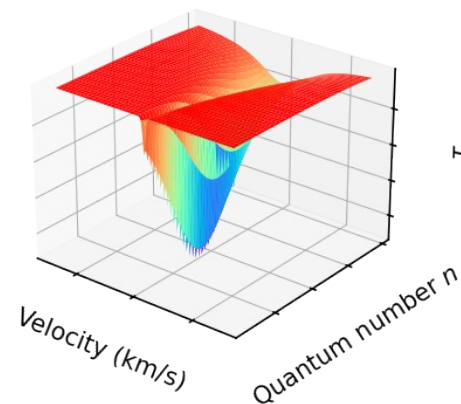
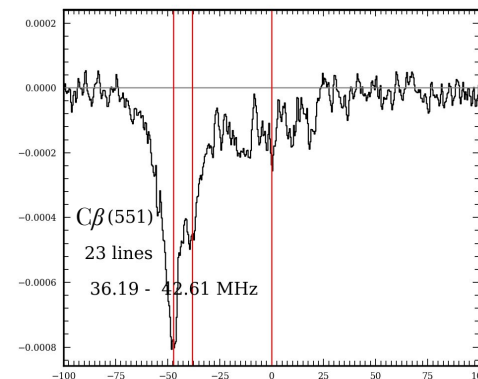
Quantum number

|                         | $T_e$ (K)       | $n_e$ ( $\text{cm}^{-3}$ ) | $T_0$ (K)      | $v_t$ (km/s)        | L (pc)         |
|-------------------------|-----------------|----------------------------|----------------|---------------------|----------------|
| <b>-47 km/s NenuFAR</b> | $39^{+7}_{-4}$  | $0.036^{+0.001}_{-0.001}$  | $2000 \pm 100$ | $3.0^{+1.2}_{-1.1}$ | $16 \pm 0.5$   |
| <b>-47 km/s LOFAR</b>   | $85 \pm 5$      | $0.040 \pm 0.005$          | $1351 \pm 83$  | $2.013 \pm 0.002$   | $35.3 \pm 1.2$ |
| <b>-38 km/s NenuFAR</b> | $43^{+4}_{-3}$  | $0.026^{+0.000}_{-0.001}$  | $1800 \pm 100$ | $4.3^{+1.1}_{-1.2}$ | $17 \pm 0.5$   |
| <b>-38 km/s LOFAR</b>   | $85 \pm 10$     | $0.040 \pm 0.005$          | $1507 \pm 128$ | $4.069 \pm 0.002$   | $18.6 \pm 1.6$ |
| <b>0 km/s</b>           | $16^{+11}_{-5}$ | $0.042^{+0.015}_{-0.016}$  | $1200 \pm 100$ | $3.0^{+1.2}_{-1.1}$ | $0.5 \pm 0.5$  |

# Perspectives

- Other transitions : C, H, He, S for  $\alpha$ ,  $\beta$ ,  $\gamma$ ,  $\delta$ ,  $\epsilon$
- 2D fitting : fitting directly the physics
  - Resolution using machine learning
- Paper in prep. : *First detections of Carbon Radio Recombination Lines with the NenuFAR telescope*

$C\beta$  towards Cas A



# Thank you for your attention !



\*Nenufar means waterlily  
in French